Climate change impacts on mycorrhizae amplify nitrogen limitation on global plant growth

Renato K. Braghiere[1,1], Joshua Fisher[2,2], Rosie A. Fisher[3,3], Mingjie Shi[4,4], Brian N Steidinger[5,5], Benjamin N Sulman[6,6], Nadia Soudzilovskaia[7,7], Xiaojuan Yang[8,8], Jingjing Liang[9,9], Kabir G Peay[5,5], Thomas W Crowther[10,10], and Richard P. Phillips[11,11]

[1]NASA Jet Propulsion Laboratory
[2]Jet Propulsion Lab
[3]National Center for Atmospheric Research (UCAR)
[4]Jet Propulsion Lab (NASA)
[5]Stanford University
[6]Oak Ridge National Laboratory
[7]Leiden University
[8]Oak Ridge National Lab
[9]Purdue University
[10]ETH Zürich
[11]Indiana University Bloomington

November 30, 2022

Abstract

Most tree species predominantly associate with a single type of mycorrhizal fungi, which can differentially affect plant nutrient acquisition and biogeochemical cycling. Here, we address for the first time the impact of mycorrhizal distributions on global carbon and nutrient cycling. Using the state-of-the-art carbon-nitrogen economics within the Community Land Model version 5 (CLM5) we found Net Primary Productivity (NPP) increased throughout the 21st century by 20%; however, as soil nitrogen has progressively become limiting, the costs to NPP for nitrogen acquisition — i.e., to mycorrhizae — have increased at a faster rate by 60%. This suggests that nutrient acquisition will increasingly demand a higher portion of assimilated carbon to support the same productivity. Uncertainties in mycorrhizal distributions are non-trivial, however, with uncertainties in NPP by up to 345 Tg C yr-1, depending on which published distribution is used. Remote sensing capabilities for mycorrhizal detection show promise for refining these estimates further.

Mycorrhizal distributions impact global patterns of carbon and nutrient cycling

R. K. Braghiere[1,2†], J. B. Fisher[1,2], R. A. Fisher[3,4], M. Shi[1,2], B. S. Steidinger[5], B. N. Sulman[6], N. A. Soudzilovskaia[7], X. Yang[6], J. Liang[8,9], K. G. Peay[5], T. W. Crowther[10], R. P. Phillips[11]

[1] Jet Propulsion Laboratory, California Institute of Technology, 4800 Oak Grove Drive, Pasadena, CA, 91109 USA.

[2] Joint Institute for Regional Earth System Science and Engineering, University of California at Los Angeles, Los Angeles, CA, 90095 USA.

[3] Climate and Global Dynamics Division, National Center for Atmospheric Research, Boulder, CO, USA.

[4] Laboratoire Évolution & Diversité Biologique, CNRS:UMR 5174, Université Paul Sabatier, Toulouse, France.

[5] Department of Biology, Stanford University, Stanford, CA, USA.

[6] Environmental Sciences Division and Climate Change Science Institute, Oak Ridge National Laboratory, Oak Ridge, TN, USA.

[7] Environmental Biology Department, Institute of Environmental Sciences, Leiden University, Leiden, The Netherlands.

[8] Department of Forestry and Natural Resources, Purdue University, West Lafayette, IN, USA.

[9] Research Center of Forest Management Engineering of State Forestry and Grassland Administration, Beijing Forestry University, Beijing, China.

[10] Department of Environmental Systems Science, ETH Zürich, Zürich, Switzerland.

[11] Department of Biology, Indiana University, 1001 E Third St, Bloomington, IN 47403, USA.

Corresponding author: Dr. Renato K. Braghiere (renato.k.braghiere@jpl.nasa.gov)

† Current address: Jet Propulsion Laboratory, M/S 233-305F, 4800 Oak Grove Drive, Pasadena, CA, 91109 USA.

Key Points:

- Global plant demand for N has increased 25% from 1850 to 2010, while the C cost associated with it has increased 60% in the same period.
- NPP has increased by 20% from 1850 to 2010, but the NPP fraction used for nitrogen acquisition increased from ~1/4 to ~1/3.
- Areas of savannas and forest-grasslands transition zones present a higher risk of nitrogen limitation to plant growth.

Keywords:

- Biogeochemistry, carbon cycling, climate change, Earth System modeling, mycorrhizae, nutrient cycling

Abstract

Most tree species predominantly associate with a single type of mycorrhizal fungi, which can differentially affect plant nutrient acquisition and biogeochemical cycling. Here, we address for the first time the impact of mycorrhizal distributions on global carbon and nutrient cycling. Using the state-of-the-art carbon-nitrogen economics within the Community Land Model version 5 (CLM5) we found Net Primary Productivity (NPP) increased throughout the 21st century by 20%; however, as soil nitrogen has progressively become limiting, the costs to NPP for nitrogen acquisition — i.e., to mycorrhizae — have increased at a faster rate by 60%. This suggests that nutrient acquisition will increasingly demand a higher portion of assimilated carbon to support the same productivity. Uncertainties in mycorrhizal distributions are non-trivial, however, with uncertainties in NPP by up to 345 Tg C yr^{-1}, depending on which published distribution is used. Remote sensing capabilities for mycorrhizal detection show promise for refining these estimates further.

Plain Language Summary

The majority of plants often join forces with specific types of fungi to improve their nutrient acquisition capacity, which ultimately impact global photosynthesis. This is the first study to explore the impacts of different types of fungi-root distributions on global carbon and nutrient cycling. Using the land component of a state-of-the-art Earth System model we found that global net carbon uptake increased throughout the 21st century by 20%, while the carbon spent on nitrogen acquisition has increased at a faster rate by 60%. This study suggests that nutrient acquisition by plants will increasingly demand a larger portion of net carbon to support the same photosynthesis.

1 Introduction

Terrestrial ecosystems have been a persistent post-industrial carbon sink, absorbing almost a third of anthropogenic carbon emissions (Ciais et al., 2013; Schimel et al., 2015; Friedlingstein et al., 2019). Studies suggest that terrestrial ecosystem productivity has increased due to elevated CO_2 concentration (Keenan et al., 2016; Zhu et al., 2016; Chen et al., 2019), but it remains unclear whether this will translate to increases in the terrestrial carbon sink in the future (Friedlingstein et al., 2006, 2014; Zhang et al., 2019). It is widely expected that limiting factors such as water (Trenberth et al., 2014; Kolus et al., 2019) and nutrients availability (Zaehle et al., 2010; Fleischer et al., 2019; Terrer et al., 2019; Wieder et al., 2015, 2019) might mediate the responses of terrestrial ecosystems to climate change. Disentangling these mechanisms and exploring the consequences of atmospheric CO_2 increase requires assessment of such mechanisms through Earth System models (ESMs), which allow comprehensive and spatially explicit assessment of the impacts of future climate on biogeochemical cycles in terrestrial ecosystems.

It has been estimated that a large part of plant nitrogen and phosphorus is provided by fungal root symbionts (van der Heijden et al., 2015), thus it is likely that mycorrhizal associations explain a large fraction of the variance in plant response to elevated CO_2 (Drake et al., 2011; Orwin et al., 2011; Kivlin et al., 2013; Sulman et al., 2017; Terrer et al., 2016, 2018). However, the global spatial distributions of these mechanisms as well as their potential impacts are still uncertain (Norby et al., 2017; Sulman et al., 2019). Only a handful of ESMs consider mycorrhizal nutrient acquisition when calculating carbon assimilation and allocation (Wang et al., 2010; Zaehle et al., 2015; Goll et al., 2017). The Community Land Model version 5 (CLM5) within the Community Earth System Model (CESM) currently enables an explicit representation of the functional differences between different types of plant symbiotic associations (Fisher et al., 2010; Brzostek et al., 2014; Shi et al., 2016; Fisher et al., 2019; Lawrence et al., 2019). However, until recently, one of the major challenges in generating global estimates of nutrient limitation on the global carbon cycle is related to a lack of understanding of the spatial distribution of nutrient-acquiring plant-microbe symbioses. Despite the availability of regional maps of present and past plant symbiotic status (Menzel et al., 2016; Swaty et al., 2016; Brundrett, 2017; Jo et al., 2019), scientists have only recently begun to develop explicit global data about mycorrhizal and nitrogen fixing associations (Davies-Barnard et al., 2020).

Recently, scientists developed methods for extrapolating spatially sparse measurements into large-scale, spatially explicit maps suitable for applications within ESMs (Shi et al., 2016; Soudzilovskaia et al., 2019; Steidinger et al., 2019; Sulman et al., 2019). These developments for the first time enable examining how mycorrhizal distributions are related to the global carbon and nitrogen cycles. In this study, we seek a better understanding of mycorrhizas on global carbon and nitrogen cycles through incorporating multiple state-of-the-art spatial distributions of mycorrhizal associations in a global ecosystem model. We first compare four existing global data products of global spatial distributions of mycorrhizal associations. Second, we perform transient global runs of CLM5 with increasing CO_2 concentration through the 20^{th} and 21^{st} centuries in order to understand the impact of the CO_2 fertilization effect combined with different spatially variable mycorrhizal representations. Finally, we evaluate the possible feedback effects that changes in spatial mycorrhizal association due to climate change (Steidinger et al., 2019) may have on the global carbon cycle.

2 Materials and Methods

2.1 Land Surface Model description: CLM5

CLM5 includes the Fixation and Uptake of Nitrogen (FUN) module calculating the carbon costs for each pathway of plant nitrogen uptake - symbiotic nitrogen fixation, direct and mycorrhizal uptake of soil nitrogen, and nitrogen retranslocation from leaves (Fisher et al., 2010; Brzostek et al., 2014; Shi et al., 2016; Allen et al., 2020). Plants shift uptake pathways to minimize the carbon costs of nitrogen uptake. FUN simulates uptake from the two major types of fungi that plants associate with: arbuscular mycorrhizal (AM) and ectomycorrhizal (ECM) fungi. Explicit representation of mycorrhizal associations improved the dynamic predictions of the nitrogen retranslocated from leaves and taken up from the soil in previous ecosystem-scale studies (Brzostek et al., 2014).

In order to generate the trade-offs between AM, ECM, and non-mycorrhizal root uptake, FUN within CLM5 uses an estimate of the percentage of aboveground biomass per grid cell that associates with each mycorrhizal type (Brzostek et al., 2014; Shi et al., 2016).

2.2 Coupling mycorrhizae spatial distribution into CLM5

Plant Functional Types (PFTs) are used to classify plants according to their physical, phylogenetic, and phenological characteristics. The value of each parameter is determined or inferred from observable characteristics. A spatial data product can be added as a 2D variable varying as function of latitude and longitude, but because land surface models also work with the concept of PFTs, adding a third dimension (i.e., latitude, longitude, and PFT) into the spatial distribution can improve accuracy of processes and reduce model uncertainty (Braghiere et al., 2019). Here, given new datasets of spatial distributions of mycorrhizal associations based on observations at different spatial resolutions, we modified CLM5 and added mycorrhizal association types per PFT within a gridcell (latitude and longitude) to also consider landscape heterogeneity within a model grid cell.

Four global maps of mycorrhizal association based on different assumptions and spatial resolutions were used to provide the percentage of ECM association (relative to AM) data for CLM5: Map A (Shi et al., 2016); Map B (Sulman et al., 2019), Map C (Steidinger et al., 2019), and Map D (Soudzilovskaia et al., 2019) (see **Fig. 1** and **Supplementary information** for details).

2.3 Simulation protocols

First, for each ECM map, initial ecosystem carbon and nitrogen stocks for 1850 were generated using a spin-up approach using 1850 concentrations of CO_2 (284.7 ppm) and the model's standard climate forcing dataset from the Global Soil Wetness Project Phase 3 version 1 (GSWP3v1) (Kim, 2017) at 1.9°x2.5° spatial resolution. The Model for Scale Adaptive River Transport (MOSART) was turned on and ice evolution on land was turned off. Model runs were performed with biogeochemistry mode on without crops for 200 years in 'accelerated decomposition' mode (see Lawrence et al. (2019) for details) by cycling through the 1901–1920 climate forcing dataset and then for 400 years in regular spin-up mode until soil and plant carbon and nitrogen stocks achieved steady state. Historical simulation was performed from 1850 to 2010 using transient GSWP3 climate, nitrogen deposition, and variable atmospheric CO_2 concentration.

Second, in order to illustrate the model sensitivity to changes in global spatial patterns of plant symbiosis due to climate change, we used a projected map of plant symbiotic status for 2070 using a relative concentration pathway (RCP) of 8.5 $W.m^{-2}$ from Steidinger et al. (2019) versus the original map with present climate (Steidinger et al., 2019). We performed future runs (2015-2070) with the biogeochemistry mode on following the Shared Socio-Economic Pathway (SSP) number 5 (Kriegler et al., 2017). SSP5 scenarios are the only ones resulting in a radiative forcing pathway as high as the highest RCP8.5 used by Steidinger et al. (2019).

The SSP5 scenario includes extreme levels of fossil fuel use, up to a doubling of global food demand, and up to a tripling of energy demand and greenhouse gas emissions over the course of the century, marking the upper end of the scenario literature in several dimensions. We used future climatological forcing from the CESM2 simulation for the CMIP6 (Lawrence et al., 2016; O'Neill et al., 2016). We used the LMWG diagnostics package from NCAR (http://github.com/NCAR/CESM_postprocessing) and Python scripts to evaluate the differences between each model run with CLM5.

2.4 Calculating nitrogen limitation

The risk of nitrogen limitation (NL) can be determined by evaluating if the growth rate of NPP used for nitrogen uptake with time is larger than the growth rate of total NPP with time. If the amount of NPP used for nitrogen uptake increases at a higher rate than the total NPP for a particular grid cell, that grid cell is considered to be at risk of spending too much carbon on nitrogen acquisition, and therefore, NL is closer to 1. On the contrary, if the amount of NPP used for nitrogen uptake increases at a lower rate than the total NPP for a particular grid cell, that area is not considered to be at risk of spending too much carbon on nitrogen acquisition. NL is calculate as:

$$NL = 1. - \frac{\propto_1(i,j)}{\propto_2(i,j)} \quad (1.0)$$

where α_1 is the slope of the linear regression of NPP used for Nitrogen uptake per gridcell (NPP_NUPTAKE(i,j)) with time and α_2 is the slope of the linear regression of NPP (NPP(i,j)) plus NPP_NUPTAKE(i,j) with time. Areas in red indicate higher risk of nitrogen limitation on NPP based on the period from 1850 to 2010.

3 Results and Discussion

3.1 Different estimates of plant symbiotic status and impacts on nitrogen uptake pathways

To better visualize the differences from maps presented in **Fig.1**, the standard deviation of the averaged difference between ECM fraction (%) of each one of the new maps and the default CLM5 map is shown in **Fig. 1e**. All three data products agree that the default map in CLM5 overestimates ECM fraction in the boreal regions, as well as drier areas of the world, such as the Atacama, Namibian, Somalian, Mongolian, Sonoran, and Australian deserts. Map C resembles the default CLM5 map A, indicating an alignment of the assumptions that climate variables are the main drivers of global biogeography of forest-tree symbioses and the proposition that fixed values of mycorrhizal associations can be prescribed following PFTs spatial distributions. The three maps disagree in the eastern USA, where map B indicates map A overestimates ECM fraction, map C indicates the opposite, and map D shows small differences. Over eastern Asia, the maps also disagree in the sign of changes of ECM fraction with respect to map A. Map B shows no particular differences in Northeast China, map C indicates that map A underestimates ECM fraction, while map D indicates the opposite. In central Europe, map C strongly (+40%) revises the default CLM5 ECM fraction upwards, while maps B and D show a much smaller positive difference in comparison to map A, except for parts of the Alps and parts of the Iberic peninsula. Given that the map A is based on PFT values, the biases in particular PFTs are presented in **Supplementary Fig. S1**.

Although all four maps agree in approximately 60% of the world area, some areas present large standard deviation values (> 30%), e.g., northern North America, throughout northern and eastern Asia, as well as parts of the tropical forests, i.e., northwest Amazon, the central part of the Congo Basin, and parts of the maritime continent. These areas would benefit from more field measurements of mycorrhizal association and further analysis.

Throughout all runs, the ECM-associated (NECM) and AM-associated (NAM) vegetation nitrogen uptake fluxes were the most impacted biogeochemical variables when including spatially explicit mycorrhizal status in CLM5, though the other nitrogen uptake pathways and their associated carbon costs were also impacted. There are four different representations of nitrogen acquisition pathways within CLM5: mycorrhizal uptake (NMYC), nitrogen fixation

(NFIX), nitrogen retranslocation from leaves (NRETRANS), and the non-mycorrhizal or direct nitrogen uptake (NNONMYC). The sum of all different nitrogen acquisition pathways is the total acquired nitrogen (TOTALN). **Table S2** shows the average carbon cost per unit of nitrogen ($gN.kgC^{-1}$) in the period 2000-2010 for each different nitrogen uptake pathway as predicted by CLM5.

On average for the period 2000-2010, the updated carbon cost per unit of nitrogen according to the three observation based maps (B,C, and D) increases 2.2%. The main areas where carbon costs of nitrogen uptake became higher are: (i) eastern North America, Europe, southeast Asia, and the tropics for mycorrhizal uptake; tropical and boreal forests for nitrogen fixation; and the tropics for nitrogen retranslocation (see **Supplementary material**). Changes in carbon costs of nitrogen acquisition via mycorrhizae uptake are 4.1% higher globally.

3.2 The effect of climate change and CO_2 fertilization on nitrogen limitation

To determine the climate change effect of nitrogen limitation on plant growth, **Fig. 2** shows the global total NPP ($PgC.yr^{-1}$), global total carbon cost of nitrogen uptake (NPP_NUPTAKE, $PgC.yr^{-1}$), global plant nitrogen demand (PLANT_NDEMAND, $TgN.yr^{-1}$), and the global total nitrogen uptake (NUPTAKE, $TgN.yr^{-1}$). Nitrogen demand is calculated as the total nitrogen that would be required if all assimilated carbon was allocated according to idealized stoichiometric ratios. The CO_2 fertilization effect, with nitrogen deposition, and climate change increased photosynthetic rates across the globe, represented by an increase in NPP from 40 $PgCyr^{-1}$ in 1850 to 47.5 $PgCyr^{-1}$ in 2010, an increase of about 20%. In turn, to support elevated productivity, plants require more nitrogen, leading to an increase in plant nitrogen demand from ~1600 $TgN.yr^{-1}$ in 1850 to 2000 $TgN.yr^{-1}$ in 2010, an increase of about 25%.

Although the rates of nitrogen uptake systematically increase in response to a higher nitrogen demand, i.e., NUPTAKE of 800 $TgN.yr^{-1}$ in 1850 to 1000 $TgN.yr^{-1}$ in 2010, the associated carbon cost of nitrogen acquisition increased at a faster rate, growing roughly 60% more expensive in 2010 (17.5 $PgCyr^{-1}$) than it was in 1850 (11.2 $PgCyr^{-1}$). In terms of the percentage of NPP spent in nitrogen acquisition, the values increased from about ~27.5% of NPP in 1850 to ~32.5% of NPP in 2010. By 2075, it is projected that the NPP used for nitrogen acquisition will reach 35% of total NPP (~22.5 $PgCyr^{-1}$), suggesting ecosystems will have much less carbon available for allocation and plant growth, possibly becoming more susceptible to

extreme events that require extra carbon for re-growth, such as droughts, fires, and insect outbreaks.

All transient runs from 1850 to 2010 with the new maps indicated a stronger effect of climate and CO_2 fertilization on nitrogen limitation compared to map A. These findings highlight that as estimated by CLM5, not only has plant demand for nitrogen increased at a faster rate than actual nitrogen uptake, but that the carbon costs associated with nitrogen acquisition have increased at a faster rate than the extra carbon gained through the CO_2 fertilization effect, i.e., plants need to invest more carbon per unit of nitrogen uptaken. This pattern is projected to continue in the future, which means that it is unlikely current plant growth rates will be sustained globally.

Fig. 3a shows the risk of nitrogen limitation (NL) calculated as described in **Eq. 1**. According to the transient runs from 1850 to 2010 using the default CLM5 map A, tropical forests have a medium to low risk of being further limited by nitrogen, which is in agreement to some studies indicating that intact ancient tropical forests tend to accumulate and recycle large quantities of nitrogen relative to temperate forests (Hedin et al., 2009).

A part of South America, Africa, and Australia, associated with savannas and forest-grassland transition zones present a higher risk of nitrogen limitation to plant growth. Parts of the temperate forests in North America, Europe, and Asia, as well as northern areas of the planet in the presence of boreal forests present a medium to high risk of nitrogen limitation.

3.3 The feedback impacts of mycorrhizal changes due to climate change

Recent evidence suggests that anthropogenic influences, primarily nitrogen deposition and fire suppression, as well as climate change have increased AM tree dominance during the past three decades in the eastern United States (Jo et al., 2019). Globally, Steidinger et al. (2019) presented a study using the same environment-mycorrhizae relationships for current climate to project potential changes in the symbiotic status of forests in the future, suggesting that projected climate for 2070 reduces the abundance of ECM trees by as much as 10%, with major changes in ECM abundance along the boreal–temperate transition zone (**Fig. 3b**).

Although the magnitude of the time lag between climate change and ecosystem responses is unknown, the predicted decline in ECM trees aligns with previous simulated warming

experiments, which have demonstrated that some important ECM hosts decline at the boreal–temperate zones under future climate conditions (Reich et al., 2015), and that ECM fungi demonstrated increased responses of mycorrhizal fungal biomass under eCO_2 compared to AM fungi (Dong et al., 2018), as the simulated response in the tropics (**Fig. 3b**).

Although it has been previously reported that climate change should impact forest symbiosis, no study has ever evaluated the potential feedback of climate change effects on mycorrhizal distribution onto nitrogen and carbon cycles. The difference in NPP for the period of 2016-2075 between the simulations using the future maps of ECM fraction and the simulations using the present-day map C (Steidinger et al., 2019) are shown in **Fig. 3c**.

Large parts of South America, especially areas associated with savannas, present the largest negative feedback effects on NPP due to future climate change impacts on mycorrhizal association, followed by areas with boreal forests. The impact over tropical forests and areas in China seem to benefit from a change in plant symbiotic status in the future. Although, these results should be interpreted carefully due to the limitation of the original forest plot training data in those areas of the globe used in Steidinger et al. (2019), machine learning algorithms indicate more ECM fungi in the tropics in the future, possibly due to the effect eCO_2 on the tropical climate.

In the SSP5-RCP8.5 runs from 2016 to 2075 with present-day plant symbiotic status, the growth rate of nitrogen uptake was 4.8 $TgN.yr^{-2}$. In terms of carbon costs, NPP is projected to increase at a rate of 265.5 $TgC.yr^{-2}$, while the carbon cost of nitrogen acquisition is projected to increase at a rate of 130.4 $TgC.yr^{-2}$, an extra 135.2 $TgC.yr^{-1}$. The feedback effect of climate change on the spatial distribution of plant symbiotic status decreases NPP globally (from 58.3 $PgC.yr^{-1}$ to 58.2 $PgC.yr^{-1}$), a negative impact of -23.1 $TgC.yr^{-1}$. The projected NPP increase rate with the future plant symbiotic status map is 266.2 $TgC.yr^{-2}$, 0.7 $TgC.yr^{-2}$ faster than the projected NPP without changes in mycorrhizae associations. However, the carbon cost of nitrogen acquisition is projected to increase at a rate of 129.1 $TgC.yr^{-2}$, versus 130.0 $TgC.yr^{-2}$ in the simulations without changes in the spatial distribution of plant symbiotic status. In terms of total NPP globally, these changes are predicted to increase carbon costs of nitrogen acquisition by 582.5 $TgC.yr^{-1}$, which significantly amplifies the effect of nutrient limitation on plant growth worldwide.

4 Conclusions

To overcome the lack of global spatial representations of mycorrhizal associations, a few studies (Soudzilovskaia et al., 2019; Steidinger et al., 2019; Sulman et al., 2019) have combined a comprehensive quantitative evaluation of mycorrhizae distribution across biomes and continents, and assembled high-resolution digital maps of the global distribution of biomass fractions of different types of mycorrhizae associations.

In our analysis, we show that differences between data products have impacts upon the nitrogen and carbon cycles in CLM5. Nonetheless, this comparison did not aim to determine which map is the most realistic. Rather, we assessed the impact of different mycorrhizal representations in CLM5 to determine signs of changes in the global nitrogen and carbon cycles. In this study, we found a negative impact on future NPP due to feedback effects of climate change and CO_2 fertilization on mycorrhizae spatial distribution.

Although the transient runs with different spatial representations of plant symbiotic status do not agree in terms of total values of nitrogen acquisition through different uptake pathways, or their relative carbon costs, all experiments using the observation based maps do agree that the increasing rate of plant nitrogen demand is higher than the rate of nitrogen uptake as previously reported. Moreover, our simulations found that the carbon costs of nitrogen acquisition also increase at a higher rate than NPP itself, indicating that plants need to invest more carbon per unit of nitrogen uptake to sustain growth at current rates globally. To our knowledge, this is the first study using observation-derived global maps of mycorrhizal association within an ESM to estimate the impacts of climate change on mycorrhizas and its feedback on the global carbon and nitrogen cycles.

Author Contributions

Conceptualization: R. K. Braghiere, J. B. Fisher, R. P. Phillips. **Formal analysis:** R. K. Braghiere, J. B. Fisher, R. A. Fisher. **Funding acquisition:** J. B. Fisher, X. Yang, J. Liang, K. G. Peay, T. W. Crowther, R. P. Phillips. **Investigation:** R. K. Braghiere, J. B. Fisher. **Methodology:** R. K. Braghiere, J. B. Fisher, R. A. Fisher, M. Shi, B. N. Sulman, N. A. Soudzilovskaia, X. Yang, R. P. Phillips. **Supervision:** J. B. Fisher, X. Yang. **Validation:** M. Shi, B. S. Steidinger, B. N. Sulman, N. A. Soudzilovskaia, J. Liang, K. G. Peay, T. W. Crowther.

Writing – original draft: R. K. Braghiere, J. B. Fisher. **Writing – review & editing:** R. K. Braghiere, J. B. Fisher, R. A. Fisher, M. Shi, B. S. Steidinger, B. N. Sulman, N. A. Soudzilovskaia, X. Yang, J. Liang, K. G. Peay, T. W. Crowther, R. P. Phillips.

Acknowledgments

This research was carried out at the Jet Propulsion Laboratory, California Institute of Technology, under a contract with the National Aeronautics and Space Administration. California Institute of Technology. Government sponsorship acknowledged. This material is based upon work supported by the U.S. Department of Energy, Office of Science, Office of Biological and Environmental Research, Terrestrial Ecosystem Science program under Award Numbers DE-SC0008317 and DE-SC0016188. Funding was also provided by the NASA IDS program. Copyright 2021. All rights reserved. We would like to acknowledge high-performance computing support from Cheyenne (NCAR, 2020) provided by NCAR's Computational and Information Systems Laboratory, sponsored by the National Science Foundation.

Data and code availability

A patch file with the modified version of CLM5 and all python scripts used for analyses and plots are available in https://doi.org/10.6084/m9.figshare.12919385.v1.

References

Allen, K., Fisher, J. B., Phillips, R. P., Powers, J. S., & Brzostek, E. R. (2020). Modeling the Carbon Cost of Plant Nitrogen and Phosphorus Uptake Across Temperate and Tropical Forests. *Frontiers in Forests and Global Change*, *3*. https://doi.org/10.3389/ffgc.2020.00043

Braghiere, R. K., Quaife, T., Black, E., He, L., & Chen, J. M. (2019). Underestimation of Global Photosynthesis in Earth System Models Due to Representation of Vegetation Structure. *Global Biogeochemical Cycles*, *33*(11), 1358–1369. https://doi.org/10.1029/2018GB006135

Brundrett, M. C. (2017). Distribution and Evolution of Mycorrhizal Types and Other Specialised Roots in Australia (pp. 361–394). https://doi.org/10.1007/978-3-319-56363-3_17

Brzostek, E. R., Fisher, J. B., & Phillips, R. P. (2014). Modeling the carbon cost of plant nitrogen

353 acquisition: Mycorrhizal trade-offs and multipath resistance uptake improve predictions of
354 retranslocation. *Journal of Geophysical Research: Biogeosciences*, *119*(8), 1684–1697.
355 https://doi.org/10.1002/2014JG002660

356 Chen, C., Park, T., Wang, X., Piao, S., Xu, B., Chaturvedi, R. K., et al. (2019). China and India
357 lead in greening of the world through land-use management. *Nature Sustainability*, *2*(2),
358 122–129. https://doi.org/10.1038/s41893-019-0220-7

359 Ciais, P., Sabine, C., Bala, G., Bopp, L., Brovkin, V., Canadell, J., et al. (2013). Carbon and
360 Other Biogeochemical Cycles. In T. F. Stocker, D. Qin, G.-K. Plattner, M. Tignor, S. K.
361 Allen, J. Boschung, et al. (Eds.), *Climate Change 2013 - The Physical Science Basis* (pp.
362 465–570). Cambridge, United Kingdom and New York, NY, USA: Cambridge University
363 Press.

364 Davies-Barnard, T., Meyerholt, J., Zaehle, S., Friedlingstein, P., Brovkin, V., Fan, Y., et al.
365 (2020). Nitrogen cycling in CMIP6 land surface models: progress and limitations.
366 *Biogeosciences*, *17*, 5129–5148. https://doi.org/10.5194/bg-17-5129-2020

367 Dong, Y., Wang, Z., Sun, H., Yang, W., & Xu, H. (2018). The Response Patterns of Arbuscular
368 Mycorrhizal and Ectomycorrhizal Symbionts Under Elevated CO2: A Meta-Analysis.
369 *Frontiers in Microbiology*, *9*. https://doi.org/10.3389/fmicb.2018.01248

370 Drake, J. E., Gallet-Budynek, A., Hofmockel, K. S., Bernhardt, E. S., Billings, S. A., Jackson, R.
371 B., et al. (2011). Increases in the flux of carbon belowground stimulate nitrogen uptake and
372 sustain the long-term enhancement of forest productivity under elevated CO2. *Ecology*
373 *Letters*, *14*(4), 349–357. https://doi.org/10.1111/j.1461-0248.2011.01593.x

374 Fisher, J. B., Sitch, S., Malhi, Y., Fisher, R. A., Huntingford, C., & Tan, S.-Y. (2010). Carbon
375 cost of plant nitrogen acquisition: A mechanistic, globally applicable model of plant
376 nitrogen uptake, retranslocation, and fixation. *Global Biogeochemical Cycles*, *24*(1), n/a-
377 n/a. https://doi.org/10.1029/2009GB003621

378 Fisher, R. A., Wieder, W. R., Sanderson, B. M., Koven, C. D., Oleson, K. W., Xu, C., et al.
379 (2019). Parametric Controls on Vegetation Responses to Biogeochemical Forcing in the

CLM5. *Journal of Advances in Modeling Earth Systems*, *11*(9), 2879–2895. https://doi.org/10.1029/2019MS001609

Fleischer, K., Rammig, A., De Kauwe, M. G., Walker, A. P., Domingues, T. F., Fuchslueger, L., et al. (2019). Amazon forest response to CO2 fertilization dependent on plant phosphorus acquisition. *Nature Geoscience*, *12*(9), 736–741. https://doi.org/10.1038/s41561-019-0404-9

Friedlingstein, P., Cox, P., Betts, R., Bopp, L., von Bloh, W., Brovkin, V., et al. (2006). Climate-carbon cycle feedback analysis: Results from the C4MIP model intercomparison. *Journal of Climate*. https://doi.org/10.1175/JCLI3800.1

Friedlingstein, P., Meinshausen, M., Arora, V. K., Jones, C. D., Anav, A., Liddicoat, S. K., & Knutti, R. (2014). Uncertainties in CMIP5 Climate Projections due to Carbon Cycle Feedbacks. *Journal of Climate*, *27*(2), 511–526. https://doi.org/10.1175/JCLI-D-12-00579.1

Friedlingstein, P., Jones, M. W., O'Sullivan, M., Andrew, R. M., Hauck, J., Peters, G. P., et al. (2019). Global Carbon Budget 2019. *Earth System Science Data*, *11*(4), 1783–1838. https://doi.org/10.5194/essd-11-1783-2019

Goll, D. S., Winkler, A. J., Raddatz, T., Dong, N., Prentice, I. C., Ciais, P., & Brovkin, V. (2017). Carbon–nitrogen interactions in idealized simulations with JSBACH (version 3.10). *Geoscientific Model Development*, *10*(5), 2009–2030. https://doi.org/10.5194/gmd-10-2009-2017

Hedin, L. O., Brookshire, E. N. J., Menge, D. N. L., & Barron, A. R. (2009). The Nitrogen Paradox in Tropical Forest Ecosystems. *Annual Review of Ecology, Evolution, and Systematics*, *40*(1), 613–635. https://doi.org/10.1146/annurev.ecolsys.37.091305.110246

van der Heijden, M. G. A., Martin, F. M., Selosse, M.-A., & Sanders, I. R. (2015). Mycorrhizal ecology and evolution: the past, the present, and the future. *New Phytologist*, *205*(4), 1406–1423. https://doi.org/10.1111/nph.13288

Jo, I., Fei, S., Oswalt, C. M., Domke, G. M., & Phillips, R. P. (2019). Shifts in dominant tree mycorrhizal associations in response to anthropogenic impacts. *Science Advances*, *5*(4),

eaav6358. https://doi.org/10.1126/sciadv.aav6358

Keenan, T. F., Prentice, I. C., Canadell, J. G., Williams, C., Wang, H., Raupach, M. R., & Collatz, G. J. (2016). Recent pause in the growth rate of atmospheric CO2 due to enhanced terrestrial carbon uptake. *Nature Communications*. https://doi.org/10.1038/ncomms13428

Kennedy, D., Swenson, S., Oleson, K. W., Lawrence, D. M., Fisher, R., Lola da Costa, A. C., & Gentine, P. (2019). Implementing Plant Hydraulics in the Community Land Model, Version 5. *Journal of Advances in Modeling Earth Systems*, *11*(2), 485–513. https://doi.org/10.1029/2018MS001500

Kim, H. (2017). Global Soil Wetness Project Phase 3 Atmospheric Boundary Conditions (Experiment 1). Data Integration and Analysis System (DIAS). https://doi.org/https://doi.org/10.20783/DIAS.501

Kivlin, S. N., Emery, S. M., & Rudgers, J. A. (2013). Fungal symbionts alter plant responses to global change. *American Journal of Botany*, *100*(7), 1445–1457. https://doi.org/10.3732/ajb.1200558

Kolus, H. R., Huntzinger, D. N., Schwalm, C. R., Fisher, J. B., McKay, N., Fang, Y., et al. (2019). Land carbon models underestimate the severity and duration of drought's impact on plant productivity. *Scientific Reports*, *9*(1), 2758. https://doi.org/10.1038/s41598-019-39373-1

Kriegler, E., Bauer, N., Popp, A., Humpenöder, F., Leimbach, M., Strefler, J., et al. (2017). Fossil-fueled development (SSP5): An energy and resource intensive scenario for the 21st century. *Global Environmental Change*, *42*, 297–315. https://doi.org/10.1016/j.gloenvcha.2016.05.015

Lawrence, D. M., Hurtt, G. C., Arneth, A., Brovkin, V., Calvin, K. V., Jones, A. D., et al. (2016). The Land Use Model Intercomparison Project (LUMIP) contribution to CMIP6: rationale and experimental design. *Geoscientific Model Development*, *9*(9), 2973–2998. https://doi.org/10.5194/gmd-9-2973-2016

Lawrence, D. M., Fisher, R. A., Koven, C. D., Oleson, K. W., Swenson, S. C., Bonan, G., et al.

(2019). The Community Land Model Version 5: Description of New Features, Benchmarking, and Impact of Forcing Uncertainty. *Journal of Advances in Modeling Earth Systems*, *11*(12), 4245–4287. https://doi.org/10.1029/2018MS001583

McGroddy, M. E., Daufresne, T., & Hedin, L. O. (2004). Scaling of C:N:P stoichiometry in forests worldwide: implications of terrestrial redfield-type ratios. *Ecology*, *85*(9), 2390–2401. https://doi.org/10.1890/03-0351

Menzel, A., Hempel, S., Manceur, A. M., Götzenberger, L., Moora, M., Rillig, M. C., et al. (2016). Distribution patterns of arbuscular mycorrhizal and non-mycorrhizal plant species in Germany. *Perspectives in Plant Ecology, Evolution and Systematics*, *21*, 78–88. https://doi.org/10.1016/j.ppees.2016.06.002

NCAR. (2019). CLM5 Documentation Release, 337.

NCAR. (2020). CHEYENNE. https://doi.org/10.5065/D6RX99HX

Norby, R. J., De Kauwe, M. G., Walker, A. P., Werner, C., Zaehle, S., & Zak, D. R. (2017). Comment on "Mycorrhizal association as a primary control of the CO 2 fertilization effect." *Science*, *355*(6323), 358.2-358. https://doi.org/10.1126/science.aai7976

O'Neill, B. C., Tebaldi, C., Van Vuuren, D. P., Eyring, V., Friedlingstein, P., Hurtt, G., et al. (2016). The Scenario Model Intercomparison Project (ScenarioMIP) for CMIP6. *Geoscientific Model Development*, *9*(9), 3461–3482. https://doi.org/10.5194/gmd-9-3461-2016

Orwin, K. H., Kirschbaum, M. U. F., St John, M. G., & Dickie, I. A. (2011). Organic nutrient uptake by mycorrhizal fungi enhances ecosystem carbon storage: a model-based assessment. *Ecology Letters*, *14*(5), 493–502. https://doi.org/10.1111/j.1461-0248.2011.01611.x

Reich, P. B., & Oleksyn, J. (2004). Global patterns of plant leaf N and P in relation to temperature and latitude. *Proceedings of the National Academy of Sciences*, *101*(30), 11001–11006. https://doi.org/10.1073/pnas.0403588101

Reich, Peter B., Sendall, K. M., Rice, K., Rich, R. L., Stefanski, A., Hobbie, S. E., & Montgomery, R. A. (2015). Geographic range predicts photosynthetic and growth response to warming in co-occurring tree species. *Nature Climate Change*, *5*(2), 148–152. https://doi.org/10.1038/nclimate2497

Riahi, K., van Vuuren, D. P., Kriegler, E., Edmonds, J., O'Neill, B. C., Fujimori, S., et al. (2017). The Shared Socioeconomic Pathways and their energy, land use, and greenhouse gas emissions implications: An overview. *Global Environmental Change*, *42*, 153–168. https://doi.org/10.1016/j.gloenvcha.2016.05.009

Schimel, D., Stephens, B. B., & Fisher, J. B. (2015). Effect of increasing CO 2 on the terrestrial carbon cycle. *Proceedings of the National Academy of Sciences*, *112*(2), 436–441. https://doi.org/10.1073/pnas.1407302112

Shi, M., Fisher, J. B., Brzostek, E. R., & Phillips, R. P. (2016). Carbon cost of plant nitrogen acquisition: global carbon cycle impact from an improved plant nitrogen cycle in the Community Land Model. *Global Change Biology*, *22*(3), 1299–1314. https://doi.org/10.1111/gcb.13131

Smith, M. R., & Myers, S. S. (2018). Impact of anthropogenic CO2 emissions on global human nutrition. *Nature Climate Change*, *8*(9), 834–839. https://doi.org/10.1038/s41558-018-0253-3

Soudzilovskaia, N. A., van Bodegom, P. M., Terrer, C., Zelfde, M. van't, McCallum, I., Luke McCormack, M., et al. (2019). Global mycorrhizal plant distribution linked to terrestrial carbon stocks. *Nature Communications*, *10*(1), 5077. https://doi.org/10.1038/s41467-019-13019-2

Steidinger, B. S., Crowther, T. W., Liang, J., Van Nuland, M. E., Werner, G. D. A., Reich, P. B., et al. (2019). Climatic controls of decomposition drive the global biogeography of forest-tree symbioses. *Nature*, *569*(7756), 404–408. https://doi.org/10.1038/s41586-019-1128-0

Sulman, B. N., Brzostek, E. R., Medici, C., Shevliakova, E., Menge, D. N. L., & Phillips, R. P. (2017). Feedbacks between plant N demand and rhizosphere priming depend on type of

mycorrhizal association. *Ecology Letters*, *20*(8), 1043–1053. https://doi.org/10.1111/ele.12802

Sulman, B. N., Shevliakova, E., Brzostek, E. R., Kivlin, S. N., Malyshev, S., Menge, D. N. L., & Zhang, X. (2019). Diverse Mycorrhizal Associations Enhance Terrestrial C Storage in a Global Model. *Global Biogeochemical Cycles*, *33*(4), 501–523. https://doi.org/10.1029/2018GB005973

Swaty, R., Michael, H. M., Deckert, R., & Gehring, C. A. (2016). Mapping the potential mycorrhizal associations of the conterminous United States of America. *Fungal Ecology*, *24*, 139–147. https://doi.org/10.1016/j.funeco.2016.05.005

Terrer, C., Vicca, S., Hungate, B. A., Phillips, R. P., & Prentice, I. C. (2016). Mycorrhizal association as a primary control of the CO 2 fertilization effect. *Science*, *353*(6294), 72–74. https://doi.org/10.1126/science.aaf4610

Terrer, C., Vicca, S., Stocker, B. D., Hungate, B. A., Phillips, R. P., Reich, P. B., et al. (2018). Ecosystem responses to elevated CO 2 governed by plant-soil interactions and the cost of nitrogen acquisition. *New Phytologist*, *217*(2), 507–522. https://doi.org/10.1111/nph.14872

Terrer, C., Jackson, R. B., Prentice, I. C., Keenan, T. F., Kaiser, C., Vicca, S., et al. (2019). Nitrogen and phosphorus constrain the CO2 fertilization of global plant biomass. *Nature Climate Change*, *9*(9), 684–689. https://doi.org/10.1038/s41558-019-0545-2

Trenberth, K. E., Dai, A., van der Schrier, G., Jones, P. D., Barichivich, J., Briffa, K. R., & Sheffield, J. (2014). Global warming and changes in drought. *Nature Climate Change*, *4*(1), 17–22. https://doi.org/10.1038/nclimate2067

Wang, Y. P., Law, R. M., & Pak, B. (2010). A global model of carbon, nitrogen and phosphorus cycles for the terrestrial biosphere. *Biogeosciences*, *7*(7), 2261–2282. https://doi.org/10.5194/bg-7-2261-2010

Wieder, W. R., Cleveland, C. C., Smith, W. K., & Todd-Brown, K. (2015). Future productivity and carbon storage limited by terrestrial nutrient availability. *Nature Geoscience*, *8*(6), 441–444. https://doi.org/10.1038/ngeo2413

514 Wieder, W. R., Lawrence, D. M., Fisher, R. A., Bonan, G. B., Cheng, S. J., Goodale, C. L., et al.
515 (2019). Beyond static benchmarking: Using experimental manipulations to evaluate land
516 model assumptions. *Global Biogeochemical Cycles*. https://doi.org/10.1029/2018GB006141

517 Zaehle, S., Friedlingstein, P., & Friend, A. D. (2010). Terrestrial nitrogen feedbacks may
518 accelerate future climate change. *Geophysical Research Letters*, *37*(1), n/a-n/a.
519 https://doi.org/10.1029/2009GL041345

520 Zaehle, S., Jones, C. D., Houlton, B., Lamarque, J.-F., & Robertson, E. (2015). Nitrogen
521 Availability Reduces CMIP5 Projections of Twenty-First-Century Land Carbon Uptake.
522 *Journal of Climate*, *28*(6), 2494–2511. https://doi.org/10.1175/JCLI-D-13-00776.1

523 Zhang, Y., Song, C., Band, L. E., & Sun, G. (2019). No Proportional Increase of Terrestrial
524 Gross Carbon Sequestration From the Greening Earth. *Journal of Geophysical Research:*
525 *Biogeosciences*, 2018JG004917. https://doi.org/10.1029/2018JG004917

526 Zhu, Z., Piao, S., Myneni, R. B., Huang, M., Zeng, Z., Canadell, J. G., et al. (2016). Greening of
527 the Earth and its drivers. *Nature Climate Change*. https://doi.org/10.1038/NCLIMATE3004

528

529

530

531

532

533

534

535

536

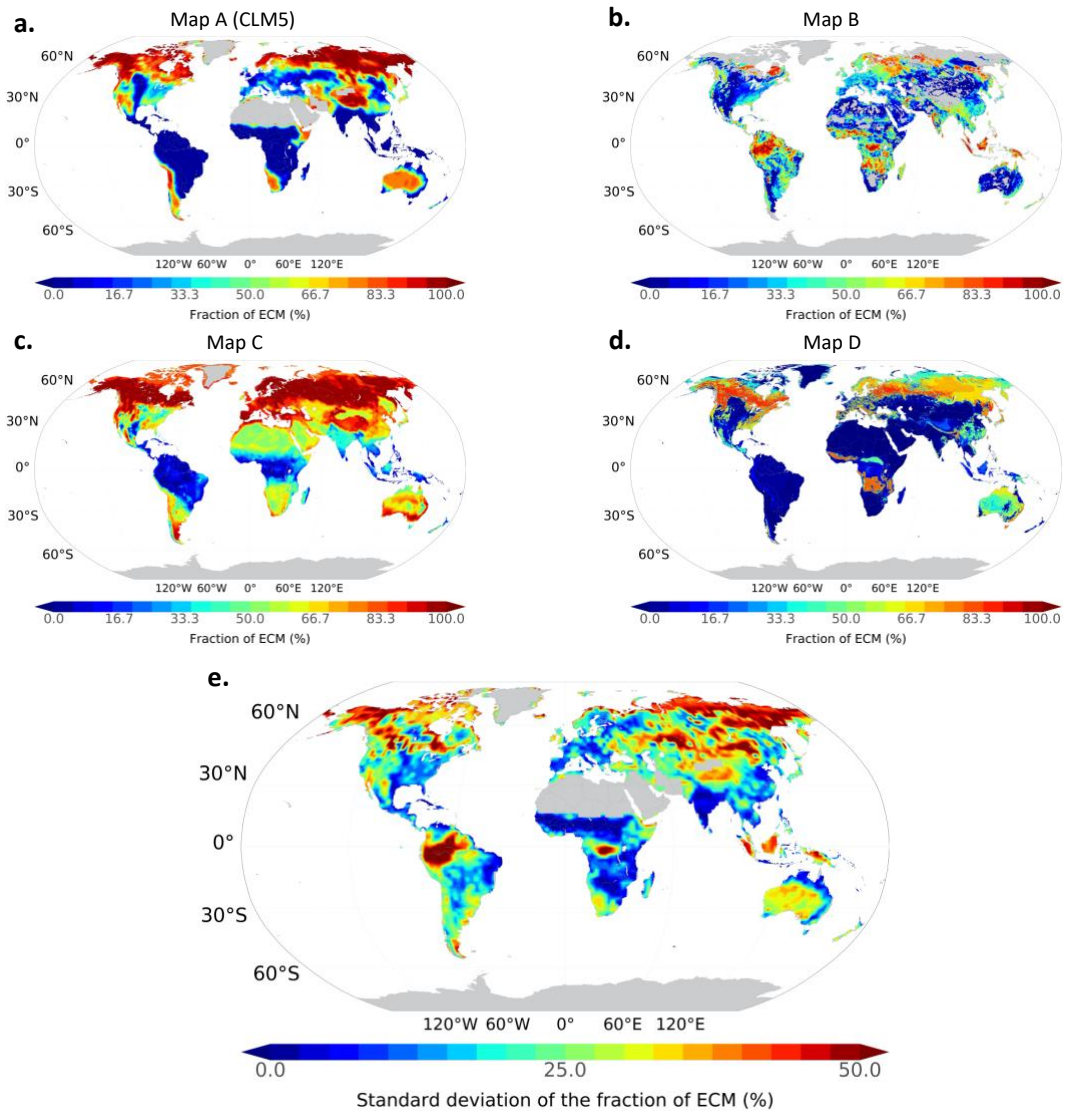

Figure 1. Global spatial distributions of ECM fraction (%). The remaining fraction is assumed to be AM. **a.** Map A (Shi et al., 2016) (look-up table x PFTs in 1.9°x2.5°); **b.** Map B (Sulman et al., 2019) (0.17°x0.17°); **c.** Map C (Steidinger et al., 2019) (1.0°x1.0° unmasked); and **d.** Map D (Soudzilovskaia et al., 2019) (0.17°x0.17°); and **e.** standard deviation of all the four maps of ECM fraction.

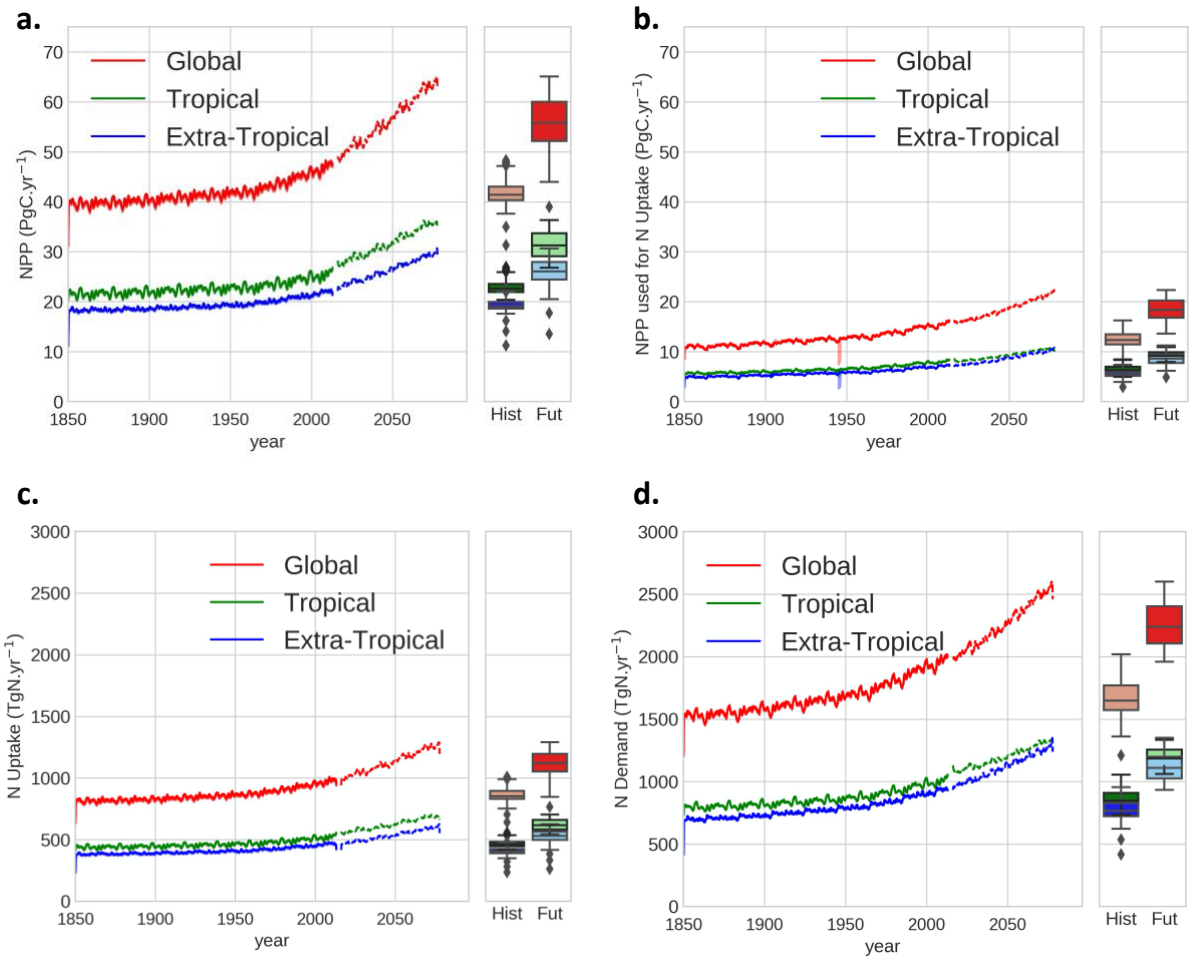

Figure 2. Trend in Net Primary Productivity and usage for nitrogen acquisition **a.** Global total NPP (PgC.yr^{-1}); **b.** global total carbon cost of nitrogen uptake (NPP_NUPTAKE, PgC.yr^{-1}); **c.** trend in nitrogen uptake and demand **a.** Global average nitrogen uptake (NUPTAKE, TgN.yr^{-1}); and **d.** global average plant nitrogen demand (PLANT_NDEMAND, TgN.yr^{-1}) for the transient historical run from 1850 to 2010 (continuous) and for the future projection SSP5 with RCP8.5 run from 2015 to 2070 (dashed) with CLM5. Tropical stands for the area of the globe between 23.5°S and 23.5°N. Extra-Tropical is the remaining area of the globe (90°S-23.5°S and 23.5°N-90°N).

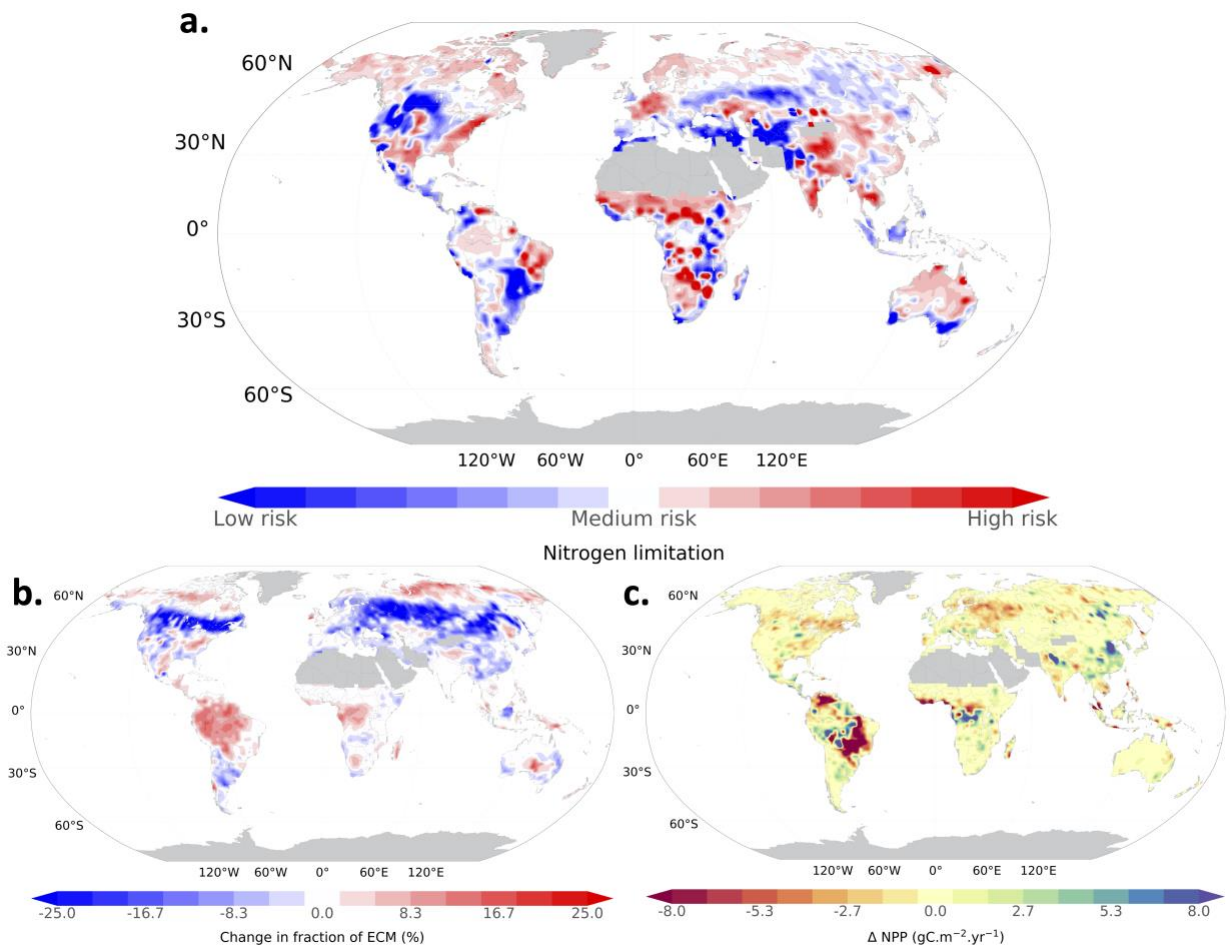

Figure 3. a. Risk of nitrogen limitation. Areas in red indicate higher risk of nitrogen limitation on NPP, and areas in blue indicate lower risk of nitrogen limitation on NPP; and projected differences in NPP and mycorrhizae driven by climate change; **b.** The impact of climate change on ECM fraction (%) derived from Steidinger et al. (2019) for 2070 following the RCP8.5 with CMIP5 simulations; **c.** Difference in NPP ($gC.m^{-2}.yr^{-1}$) for future simulations (2016-2075) between projected future map generated for the year of 2070 and the present-day map C (Steidinger et al., 2019). The projected runs with CLM5 followed the SSP5 scenario in combination with RCP8.5 climate forcing from CESM, member of CMIP6 simulations.

Mycorrhizal distributions impact global patterns of carbon and nutrient cycling

R. K. Braghiere[1,2†], J. B. Fisher[1,2], R. A. Fisher[3,4], M. Shi[1,2], B. S. Steidinger[5], B. N. Sulman[6], N. A. Soudzilovskaia[7], X. Yang[6], J. Liang[8,9], K. G. Peay[5], T. W. Crowther[10], R. P. Phillips[11]

[1] Jet Propulsion Laboratory, California Institute of Technology, 4800 Oak Grove Drive, Pasadena, CA, 91109 USA.

[2] Joint Institute for Regional Earth System Science and Engineering, University of California at Los Angeles, Los Angeles, CA, 90095 USA.

[3] Climate and Global Dynamics Division, National Center for Atmospheric Research, Boulder, CO, USA.

[4] Laboratoire Évolution & Diversité Biologique, CNRS:UMR 5174, Université Paul Sabatier, Toulouse, France.

[5] Department of Biology, Stanford University, Stanford, CA, USA.

[6] Environmental Sciences Division and Climate Change Science Institute, Oak Ridge National Laboratory, Oak Ridge, TN, USA.

[7] Environmental Biology Department, Institute of Environmental Sciences, Leiden University, Leiden, The Netherlands.

[8] Department of Forestry and Natural Resources, Purdue University, West Lafayette, IN, USA.

[9] Research Center of Forest Management Engineering of State Forestry and Grassland Administration, Beijing Forestry University, Beijing, China.

[10] Department of Environmental Systems Science, ETH Zürich, Zürich, Switzerland.

[11] Department of Biology, Indiana University, 1001 E Third St, Bloomington, IN 47403, USA.

Corresponding author: Dr. Renato K. Braghiere (renato.k.braghiere@jpl.nasa.gov)

† Current address: Jet Propulsion Laboratory, M/S 233-305F, 4800 Oak Grove Drive, Pasadena, CA, 91109 USA.

Supplementary Materials Document

Includes:

- Supplementary Information
- Supplementary Tables
- Supplementary Figures
- Supplementary References

Supplementary information

Land Surface model description: the Community Land Model version 5 (CLM5)

CLM5 is the land surface component of the Community Earth System Model 2 (CESM2; https://www.cesm.ucar.edu/models/cesm2/). CLM5 includes three important changes to the representation of plant carbon and nitrogen dynamics: i) the Leaf Utilization of Nitrogen for Assimilation (LUNA) module allows plants to adjust their partitioning of nitrogen among the maximum rate of carboxylation (V_{cmax}), the maximum rate of electron transport (J_{max}), and other leaf nitrogen components, to achieve co-limitation of photosynthesis under the prevailing time-averaged environmental drivers (CO_2, temperature, humidity, soil moisture, radiation, and day length) (Xu et al., 2012; Ali et al., 2016; Fisher et al., 2019); ii) the 'FlexCN' module allows plants to alter and optimize their stoichiometry, removing the down-regulation of gross primary productivity (GPP) that was used in CLM4 and CLM4.5 (Cheng et al., 2019; Ghimire et al., 2016). In the new allocation algorithm, the total nitrogen supply in each timestep is partitioned among tissues in proportion to their relative 'demand' terms. Additional details on how stoichiometry is optimized can be found in Lawrence et al. (2019) and Fisher et al. (2019); and finally, iii) the Fixation and Uptake of Nitrogen (FUN) module implements a 'carbon cost' for each source of plant nitrogen uptake (Fisher et al., 2010; Brzostek et al., 2014; Shi et al., 2016; Allen et al., 2020).

The carbon cost of nitrogen uptake from soil by mycorrhizal or non-mycorrhizal pathways, for each soil layer j, is controlled by two uptake parameters that pertain respectively to the relationship between soil nitrogen and nitrogen uptake, and between fine root carbon density and nitrogen uptake. For mycorrhizal or non-mycorrhizal nitrogen uptake, the cost functions are given as:

$$N_{cost,pathway,j} = \frac{k_{n,pathway}}{N_{smin,j}} + \frac{k_{c,pathway}}{c_{root,j}} \quad (1.0)$$

where $k_{n,\text{pathway}}$ (kgC.m^{-2}) and $k_{\text{c,pathway}}$ (kgC.m^{-2}) varies according to whether the pathway considered is referring to a non-mycorrhizal (direct), ECM, or AM uptake. $N_{smin,j}$ and $c_{root,j}$ are the soil nitrogen content (gN.m^{-3}) and fine root carbon density (gC.m^{-3}), respectively. Please refer to CLM5 technical note and related publications (Fisher et al., 2019; Lawrence et al., 2019; NCAR, 2019) for the complete set of equations.

Shi et al. (2016) classified the Plant Functional Types (PFTs) in CLM, based upon known associations between plant species and either arbuscular mycorrhizae (AM) or ectomycorrhizae (ECM) fungi described in the literature (Read, 1991; Allen et al., 1995; Phillips et al., 2013). While some PFTs are usually AM-dominated (e.g., grasslands), others are usually ECM-dominated (e.g., boreal forest). PFT symbiont fraction estimates are available as ratios of the AM-associated and ECM-associated plants of the CLM PFTs as a table in Shi et al. (2016). These numbers are usually binary, associating one PFT with a single type of mycorrhizae, e.g., 0% or 100%, except for broadleaf deciduous temperate trees, which associates 50% with AM and 50% with ECM.

Coupling mycorrhizae spatial distribution into CLM5

In CLM5, within each grid cell, the soil area available for vegetation is divided into patches that correspond to the area fraction of that PFT. For each PFT, a number of key parameters are defined, such as the target tissue C:N values, stomatal water use efficiency, maximum hydraulic conductivity and sensitivity to embolism (Kennedy et al., 2019), tissue allocation fractions (for leaves, fine roots, stem, and coarse roots), tissue turnover times, and the rate at which litter class (labile, lignin, cellulose) decays and returns nutrients to the soil after death. Four global maps of mycorrhizal association based on different assumptions and spatial resolutions were added into CLM5 to provide the percentage of ECM association (relative to

AM) data for CLM5: Map A (Shi et al., 2016); Map B (Sulman et al., 2019), Map C (Steidinger et al., 2019), and Map D (Soudzilovskaia et al., 2019) (**Fig. 1**).

Map B was derived from Sulman et al. (2019), who assembled empirical AM data points presenting species number of AM fungi obtained from the MAARJAM database (Öpik et al., 2010), and ECM data points presenting species number of ECM fungi obtained from Tedersoo et al. (2014). These data were used to define niche models which were used to develop spatial maps of the relative probability of AM and ECM fungal presence within areal units of 10 arcmin. These niche models were used to estimate ECM fraction by comparing the relative probability of AM and ECM presence:

$$\%ECM = 100*p(ECM)/(p(ECM) + p(AM)) \quad (2.0)$$

where p(ECM) and p(AM) are the probabilities of ECM or AM presence, respectively, from the niche model in each grid cell.

Map C was derived from Steidinger et al. (2019), who proposed a global map of the symbiotic status of forests, using a database of over 1 million forest inventory plots containing more than 28,000 tree species, and 70 global predictor layers: 19 climatic indices (relating to annual, monthly, and quarterly temperature and precipitation variables), 14 soil chemical indices (relating to soil nitrogen density, microbial nitrogen, C:N ratios and soil P fractions, pH and cation exchange capacity), 26 vegetative indices (relating to leaf area index, total stem density, enhanced vegetation index means and variances), and 5 topographic variables (relating to elevation and hillshade). Their maps provide quantitative estimates of the distribution of aboveground biomass fractions among AM, ECM, and N fixers plants within areal units of 0.5° and 1.0°.

Map D was proposed by Soudzilovskaia et al. (2019), who assembled a global database on plant mycorrhizal type associations that included 2,169 studies and 27,736 species-by-site records for 12,702 plant species and combined it with information about dominant plant species and their growth form across distinct combinations of Bailey's with 98 ecoregions (Bailey, 2014) and European Space Agency (ESA) land cover categories (ESA, 2017) with spatial resolution of 300 m. Their maps provide quantitative estimates of the distribution of aboveground biomass fractions among AM, ECM, and ericoid mycorrhiza (ERM) plants withins areal units of 10 arcmin.

The maps D and B are principally different from maps A and C. Consequently, conversions to unify the data for comparisons have to be applied. Map D shows fractions of biomass for all plants, not only trees, while the map B shows the likelihood of occurrence of ECM biomass in a grid cell based on a species distribution model fit to a genomic database. Sulman et al. (2019) produced a range from very low likelihood of ECM fungal DNA being present in observations to higher likelihood of ECM presence. In order to compare map B with other maps, the ECM map was first combined with the AM map and normalized, producing a spectrum that incorporates both mycorrhizal types.

A regridding process of the maps to CLM5 grid scales was applied by calculating an average value for ECM in percentage per PFT per gridcell based on the GLC2000 land cover data (Bartholomé & Belward, 2005) at a spatial resolution of 500 m following a look-up table (**Supplementary Table S1**). The average value of ECM percentage was assigned to one of the 16 particular natural vegetation PFTs in CLM5 per gridcell, assuming that AM and ECM trees do not differ in biomass. In this case, using basal area maps and biomass percentages map interchangeably is acceptable in tree-dominated areas. In other areas, it is assumed that although differences in the data products might exist, the nature of the measure is assumed to have little impact, as long as given in the format of a ratio of ECM over ECM plus AM present in the grid cells, due to the fact that CLM5 ingests the data as a ECM ratio per PFT.

Table S1. Look-up table between GLC Global Class and CLM PFTs.

CLM PFT	Classification	GLC Global Class
PFT 0	Bare soil (not vegetated)	(19)Bare Areas
PFT 1	Needleleaf evergreen temperate tree	(04)Tree Cover, needle-leaved, evergreen; (06)Tree Cover, mixed leaf type; (07)Tree Cover, regularly flooded, fresh water (& brackish); (08)Tree Cover, regularly flooded, saline water; (09)Mosaic; (10)Tree Cover, burnt; (17)Mosaic;

PFT 2	Needleleaf evergreen boreal tree	(04)Tree Cover, needle-leaved, evergreen; (06)Tree Cover, mixed leaf type; (07)Tree Cover, regularly flooded, fresh water (& brackish); (08)Tree Cover, regularly flooded, saline water; (09)Mosaic; (10)Tree Cover, burnt; (17)Mosaic;
PFT 3	Needleleaf deciduous boreal tree	(05)Tree Cover, needle-leaved, deciduous; (06)Tree Cover, mixed leaf type; (07)Tree Cover, regularly flooded, fresh water (& brackish); (08)Tree Cover, regularly flooded, saline water; (09)Mosaic; (10)Tree Cover, burnt; (17)Mosaic;
PFT 4	Broadleaf evergreen tropical tree	(01) Tree Cover, broadleaved, evergreen; (06)Tree Cover, mixed leaf type; (07)Tree Cover, regularly flooded, fresh water (& brackish); (08)Tree Cover, regularly flooded, saline water; (09)Mosaic; (10)Tree Cover, burnt; (17)Mosaic;
PFT 5	Broadleaf evergreen temperate tree	(01) Tree Cover, broadleaved, evergreen; (06)Tree Cover, mixed leaf type; (07)Tree Cover, regularly flooded, fresh water (& brackish); (08)Tree Cover, regularly flooded, saline water; (09)Mosaic; (10)Tree Cover, burnt; (17)Mosaic;
PFT 6	Broadleaf deciduous tropical tree	(02)Tree Cover, broadleaved, deciduous, closed; (06)Tree Cover, mixed leaf type; (07)Tree Cover, regularly flooded, fresh water (& brackish); (08)Tree Cover, regularly flooded, saline water; (09)Mosaic; (10)Tree Cover, burnt; (17)Mosaic;
PFT 7	Broadleaf deciduous temperate tree	(02)Tree Cover, broadleaved, deciduous, closed; (06)Tree Cover, mixed leaf type; (07)Tree Cover, regularly flooded, fresh water (& brackish); (08)Tree Cover, regularly flooded, saline water; (09)Mosaic; (10)Tree Cover, burnt; (17)Mosaic;
PFT 8	Broadleaf deciduous boreal tree	(02)Tree Cover, broadleaved, deciduous, closed; (06)Tree Cover, mixed leaf type; (07)Tree Cover, regularly flooded, fresh water (& brackish); (08)Tree Cover, regularly flooded, saline water; (09)Mosaic; (10)Tree Cover, burnt; (17)Mosaic;

PFT 9	Broadleaf evergreen shrub	(01) Tree Cover, broadleaved, evergreen; (06)Tree Cover, mixed leaf type; (09)Mosaic; (11)Shrub Cover, closed-open, evergreen; (13)Herbaceous Cover, closed-open; (14)Sparse Herbaceous or sparse Shrub Cover; (15)Regularly flooded Shrub and/or Herbaceous Cover; (17)Mosaic; (18)Mosaic
PFT 10	Broadleaf deciduous temperate shrub	(03)Tree Cover, broadleaved, deciduous, open; (06)Tree Cover, mixed leaf type; (09)Mosaic; (12)Shrub Cover, closed-open, deciduous; (13)Herbaceous Cover, closed-open; (14)Sparse Herbaceous or sparse Shrub Cover; (15)Regularly flooded Shrub and/or Herbaceous Cover; (17)Mosaic; (18)Mosaic
PFT 11	Broadleaf deciduous boreal shrub	(03)Tree Cover, broadleaved, deciduous, open; (06)Tree Cover, mixed leaf type; (09)Mosaic; (12)Shrub Cover, closed-open, deciduous; (13)Herbaceous Cover, closed-open; (14)Sparse Herbaceous or sparse Shrub Cover; (15)Regularly flooded Shrub and/or Herbaceous Cover; (17)Mosaic; (18)Mosaic
PFT 12	C3 arctic grass	(09)Mosaic; (13)Herbaceous Cover, closed-open; (14)Sparse Herbaceous or sparse Shrub Cover; (15)Regularly flooded Shrub and/or Herbaceous Cover; (17)Mosaic; (18)Mosaic
PFT 13	C3 nonarctic grass	(09)Mosaic; (13)Herbaceous Cover, closed-open; (14)Sparse Herbaceous or sparse Shrub Cover; (15)Regularly flooded Shrub and/or Herbaceous Cover; (17)Mosaic; (18)Mosaic
PFT 14	C4 grass	(09)Mosaic; (13)Herbaceous Cover, closed-open; (14)Sparse Herbaceous or sparse Shrub Cover; (15)Regularly flooded Shrub and/or Herbaceous Cover; (17)Mosaic; (18)Mosaic
PFT 15	Corn	(09)Mosaic; (16)Cultivated and managed areas; (17)Mosaic; (18)Mosaic

PFT 16	Wheat	(09)Mosaic; (16)Cultivated and managed areas; (17)Mosaic; (18)Mosaic
PFT 17	NaN	(20)Water Bodies (natural & artificial); (21)Snow and Ice (natural & artificial); (22)Artificial surfaces and associated areas; (23)No data

*****(09) Mosaic: Tree cover / Other natural vegetation; (17) Mosaic: Cropland / Tree Cover / Other natural vegetation; (18) Mosaic: Cropland / Shrub or Grass Cover.

Table S2. Average carbon cost values per unit nitrogen ($gN.kgC^{-1}$) from 2000 to 2010 for each different pathway and sum for all new maps and the default one in CLM5.

Pathway cost	**Reference**	**TRANSIENT – 2000 – 2010**				
(gN.kgC^{-1})	**Map A (CLM5)**	**Map B**	**Map C**	**Map D**	**Average (B,C,D)**	**Change (%)**
NMYC	1.15	1.15	1.21	1.04	1.13	1.4%
NFIX	104.00	103.80	105.20	107.60	105.53	-1.5%
NRETRANS	925.00	924.00	905.00	914.00	914.33	1.2%
NNONMYC	115.53	115.13	130.00	124.97	123.01	-6.5%
TOTALN	38.33	38.07	36.62	37.82	37.50	2.2%

Table S3. Average values from 2000 to 2010 of nitrogen uptake for each one of the different pathways and sum for the spatially distributed PFT based.

2000-2010

Pathway	**Reference**	**TRANSIENT – 2000 – 2010**		
(TgNyr-1)	**Map A (CLM5)**	**Map B**	**Map C**	**Map D**
NECM	10.7	10.8	14.8	7.5
NAM	9.9	9.8	8.7	11.8
NFIX	52.0	51.9	52.6	53.8

NRETRANS	92.5	92.4	90.5	91.4
NNONMYC	808.7	805.9	793.0	799.8
TOTALN	973.7	970.8	959.5	964.4

144

145

146

147

148

149 **Table S4.** Average values from 2000 to 2010 of carbon costs of nitrogen uptake for each one of
150 the different pathways and sum for the spatially distributed PFT based. The values of CLM4-
151 FUN from Shi et al. (2016) are shown as reference.

	1995-2004	***2000-2010***			
Pathway	**Reference**	**Reference**	**TRANSIENT - 2000 - 2010**		
(PgCyr-1)	**CLM4-FUN**	**Map A (CLM5)**	**Map B**	**Map C**	**Map D**
NPP_MYC	1.2	17.9	17.9	19.4	18.6
NPP_NFIX	0.4	0.5	0.5	0.5	0.5
NPP_NRETRANS	0.6	0.1	0.1	0.1	0.1
NPP_TOTAL N	2.4	25.4	25.5	26.2	25.5
NPP_NPASSIVE	0.0	0.0	0.0	0.0	0.0
NPP_NDIRECT	0.2	7.0	7.0	6.1	6.4

152

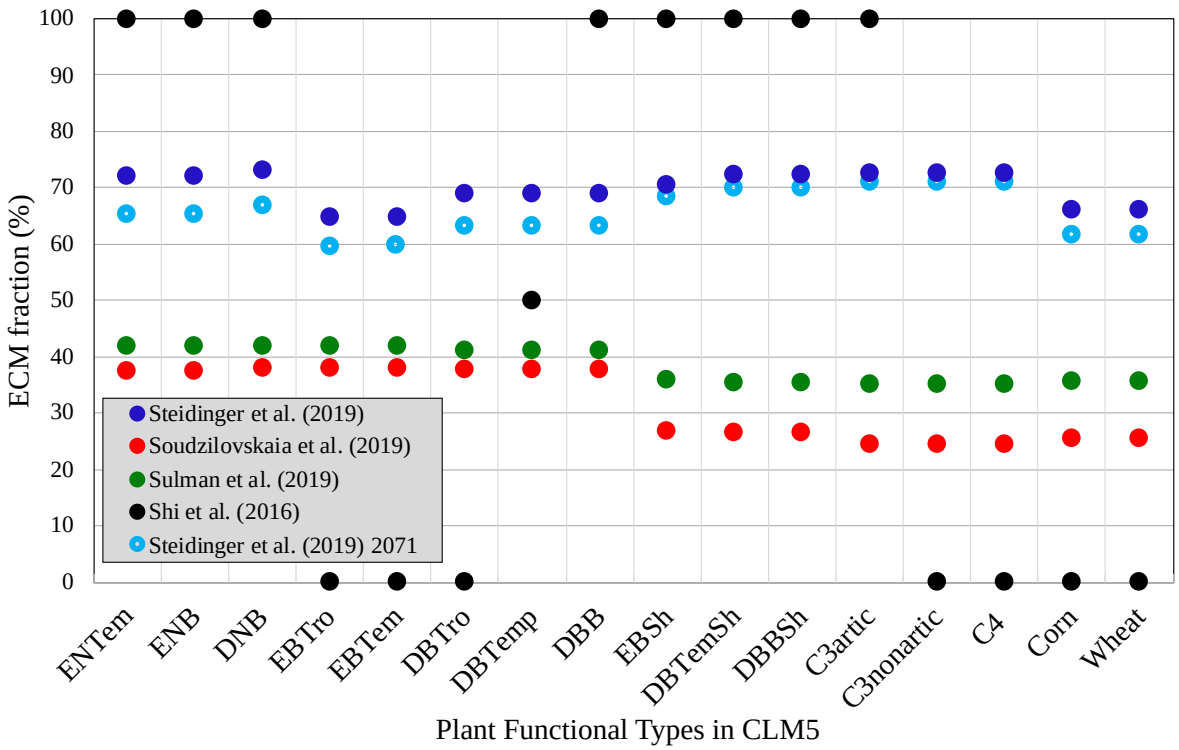

Figure S1. PFT global average of ECM fraction in percentage for ref. (Sulman et al., 2019); ref. (Steidinger et al., 2019) present and future (2071); ref. (Soudzilovskaia et al., 2019) and the base map in CLM5 as in ref. (Shi et al., 2016).

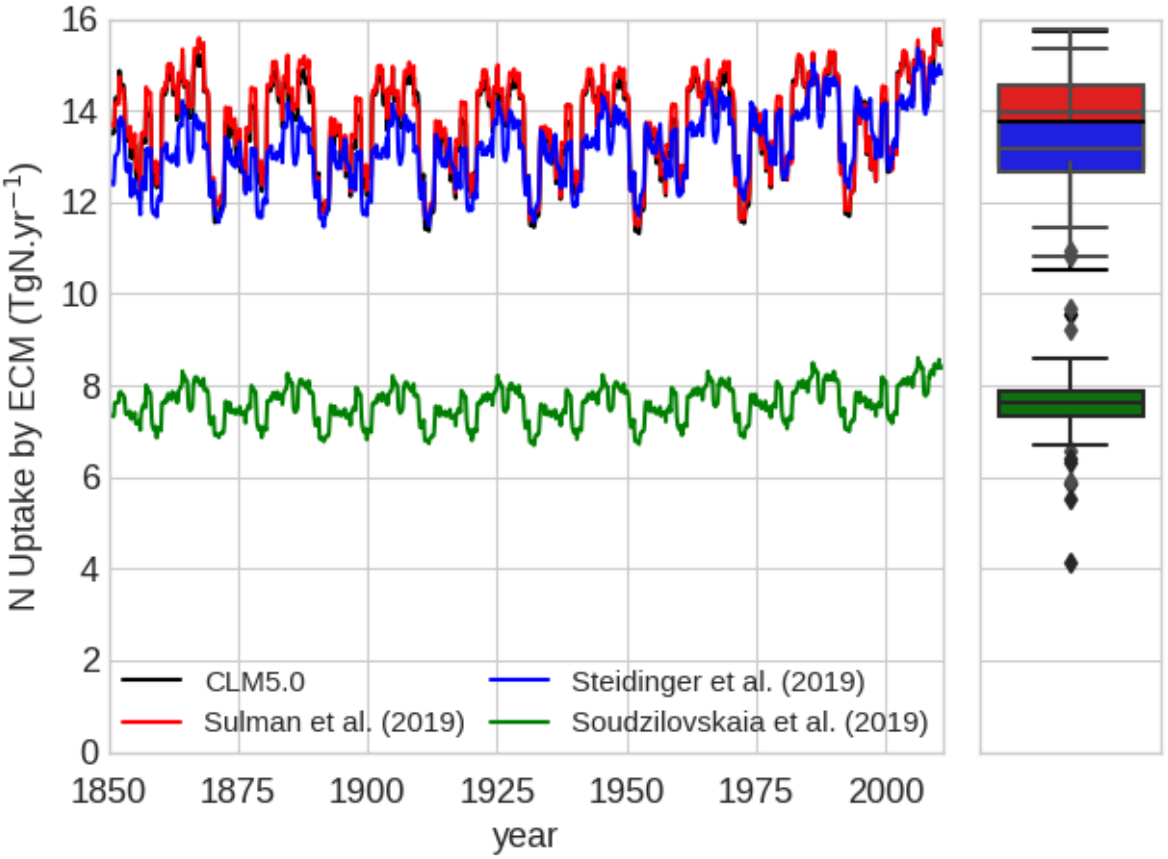

Figure S2. Nitrogen uptake through ectomycorrhizal association (NECM) in TgNyr^{-1} for the transient run (1850-2010) for ref. (Sulman et al., 2019); ref. (Steidinger et al., 2019); and ref. (Soudzilovskaia et al., 2019) and the base map in CLM5 as in ref. (Shi et al., 2016) based on fixed PFT values.

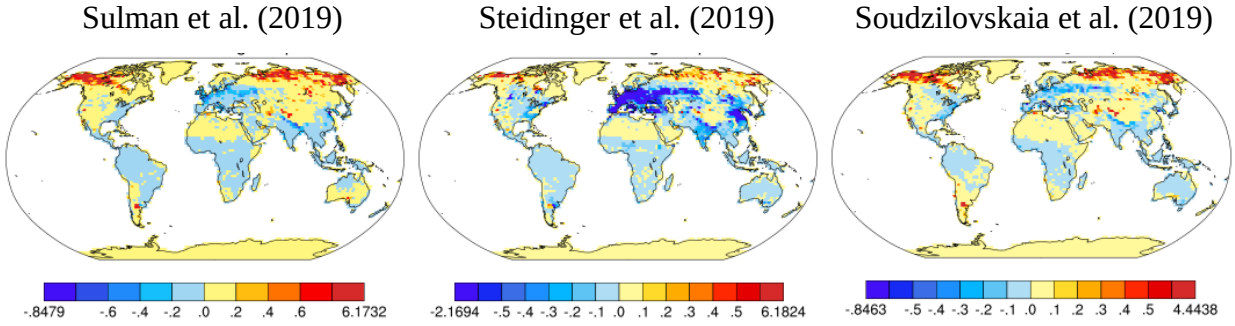

Figure S3. Revised global AM N uptake ($gNm^{-2}y^{-1}$) spatial distribution between **a.** Sulman et al. (2019); **b.** Steidinger et al. (2019); and **c.** Soudzilovskaia et al. (2019) and the base map in CLM5 as in Shi et al. (2016) based on PFT values per grid cell.

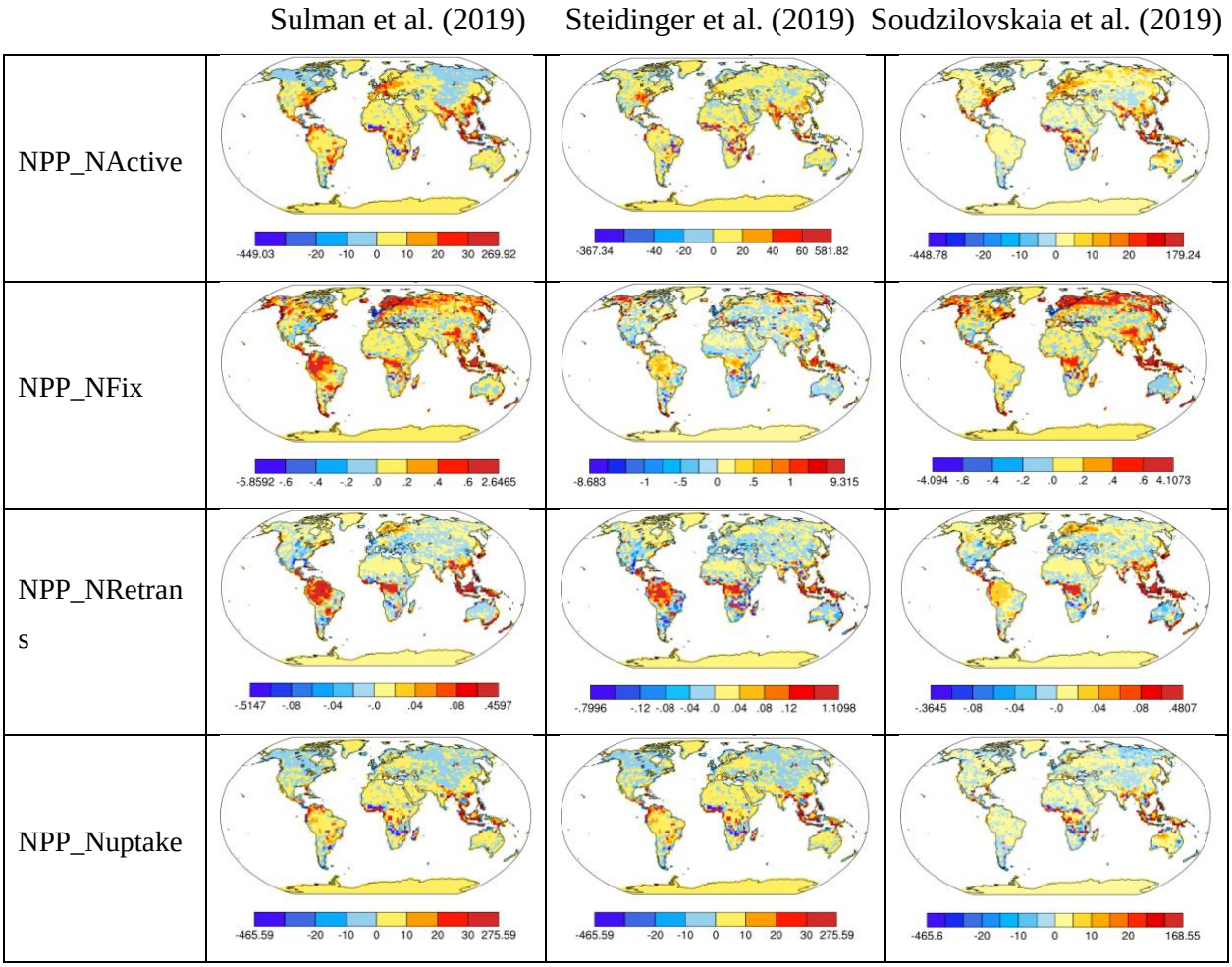

Figure S4. Revised carbon used for nitrogen uptake ($gCm^{-2}y^{-1}$) spatial distribution between a. Sulman et al. (2019); b. Steidinger et al. (2019); and c. Soudzilovskaia et al. (2019) and the base

map in CLM as in Shi et al. (2016) based on PFT values per gridbox for different pathways: Mycorrhizal (NPP_NActive), Symbiotic BNF (NPP_NFix), retranslocated N (NPP_NRetrans), and total (NPP_Nuptake).

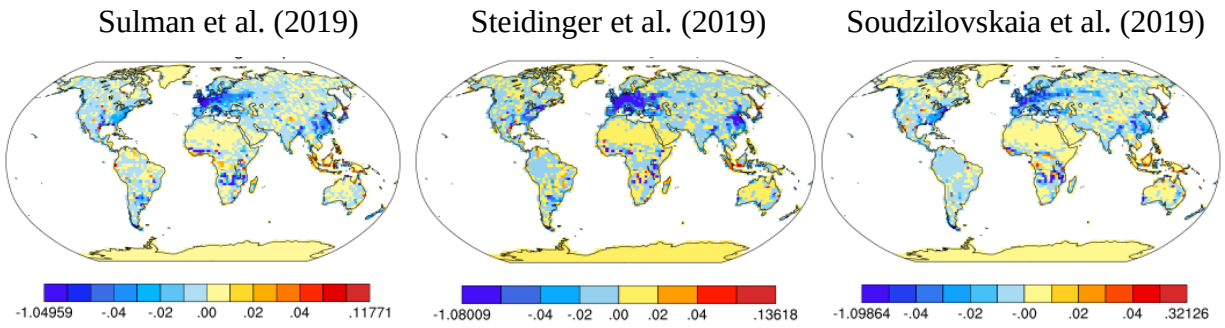

Figure S5. Revised Autotrophic Respiration ($gCm^{-2}y^{-1}$) spatial distribution between **a.** Sulman et al. (2019); **b.** Steidinger et al. (2019); and **c.** Soudzilovskaia et al. (2019) and the base map in CLM as in Shi et al. (2016) based on fixed PFT values (**above**) and based on PFT values per gridbox (**below**).

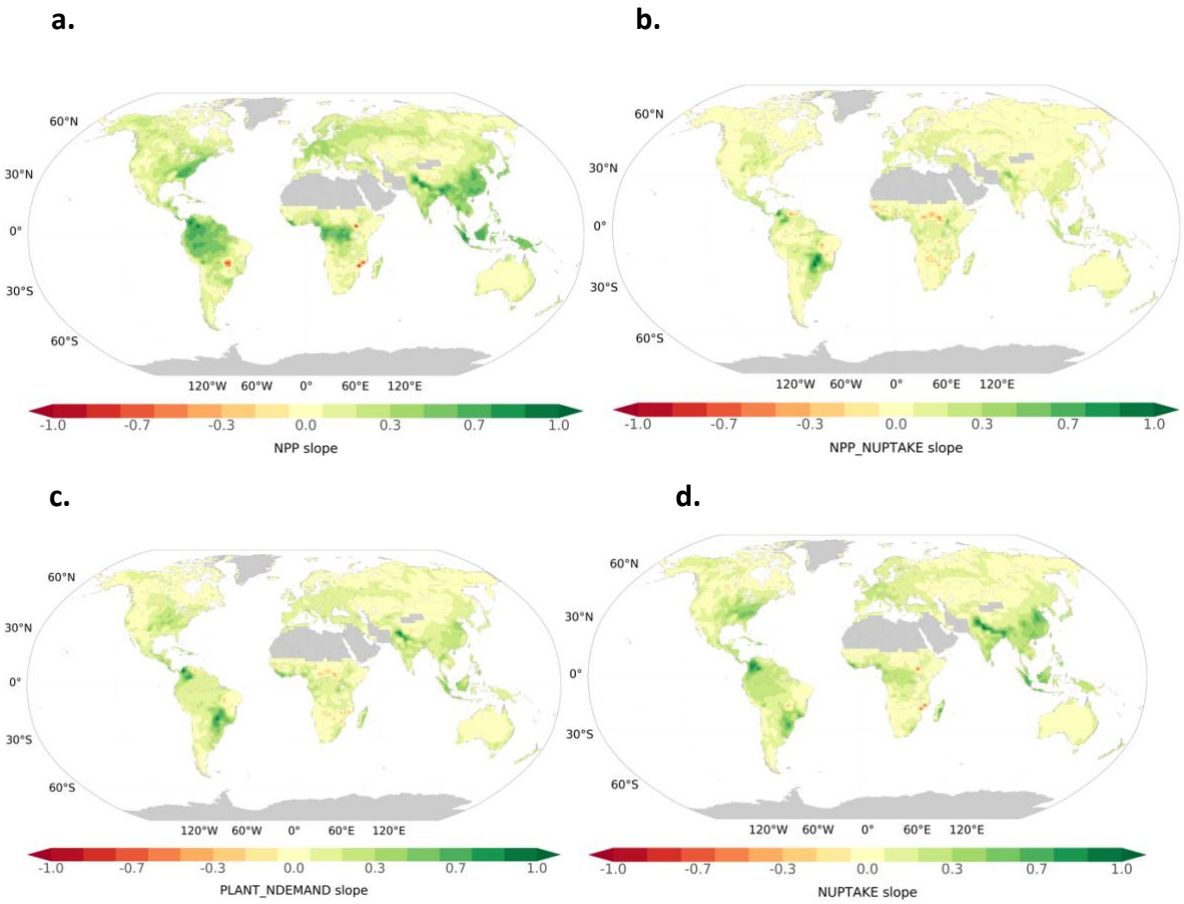

Figure S6. Normalized linear regression slope of **a.** NPP, **b.** NPP_NUPTAKE, **c.** PLANT_NDEMAND, and **d.** NUPTAKE with time.

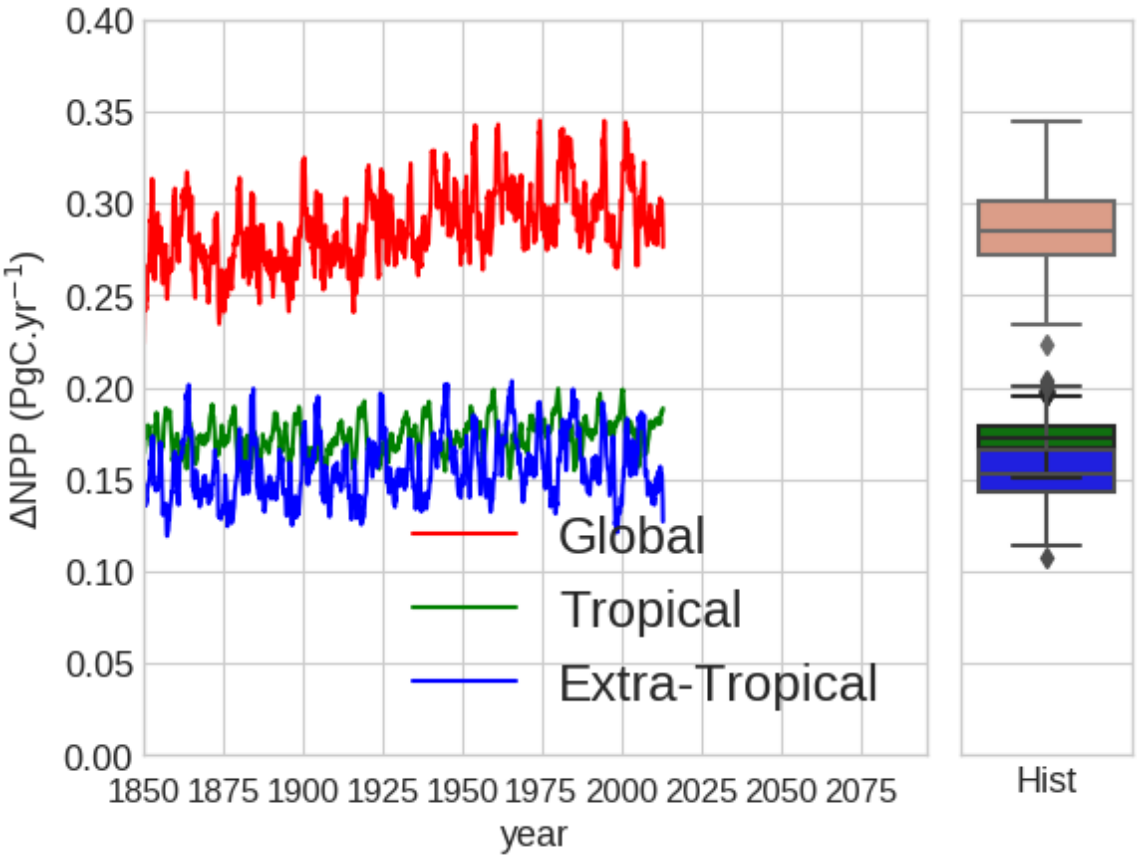

Figure S7. Global average maximum ΔNPP (PgC.yr^{-1}) for the transient historical runs from 1850 to 2010 with CLM5 for all different ECM maps.

References

Ali, A. A., Xu, C., Rogers, A., Fisher, R. A., Wullschleger, S. D., Massoud, E. C., et al. (2016). A global scale mechanistic model of photosynthetic capacity (LUNA V1.0). *Geoscientific Model Development*, *9*(2), 587–606. https://doi.org/10.5194/gmd-9-587-2016

Allen, E. B., Allen, M. F., Helm, D. J., Trappe, J. M., Molina, R., & Rincon, E. (1995). Patterns and regulation of mycorrhizal plant and fungal diversity. *Plant and Soil*, *170*(1), 47–62. https://doi.org/10.1007/BF02183054

Allen, K., Fisher, J. B., Phillips, R. P., Powers, J. S., & Brzostek, E. R. (2020). Modeling the Carbon Cost of Plant Nitrogen and Phosphorus Uptake Across Temperate and Tropical Forests. *Frontiers in Forests and Global Change*, *3*. https://doi.org/10.3389/ffgc.2020.00043

Bailey, R. G. (2014). *Ecoregions: The ecosystem geography of the oceans and continents*. *Ecoregions: The Ecosystem Geography of the Oceans and Continents*. Springer New York. https://doi.org/10.1007/978-1-4939-0524-9

Bartholomé, E., & Belward, A. S. (2005). GLC2000: a new approach to global land cover mapping from Earth observation data. *International Journal of Remote Sensing*. https://doi.org/10.1080/01431160412331291297

Braghiere, R. K., Quaife, T., Black, E., He, L., & Chen, J. M. (2019). Underestimation of Global Photosynthesis in Earth System Models Due to Representation of Vegetation Structure. *Global Biogeochemical Cycles*, *33*(11), 1358–1369. https://doi.org/10.1029/2018GB006135

Brzostek, E. R., Fisher, J. B., & Phillips, R. P. (2014). Modeling the carbon cost of plant nitrogen acquisition: Mycorrhizal trade-offs and multipath resistance uptake improve predictions of retranslocation. *Journal of Geophysical Research: Biogeosciences*, *119*(8), 1684–1697. https://doi.org/10.1002/2014JG002660

Cheng, S. J., Hess, P. G., Wieder, W. R., Thomas, R. Q., Nadelhoffer, K. J., Vira, J., et al. (2019). Decadal fates and impacts of nitrogen additions on temperate forest carbon storage: a data–model comparison. *Biogeosciences*, *16*(13), 2771–2793. https://doi.org/10.5194/bg-16-2771-2019

ESA. (2017). CCI Land cover map 2015.

Fisher, J. B., Sitch, S., Malhi, Y., Fisher, R. A., Huntingford, C., & Tan, S.-Y. (2010). Carbon cost of plant nitrogen acquisition: A mechanistic, globally applicable model of plant

nitrogen uptake, retranslocation, and fixation. *Global Biogeochemical Cycles*, *24*(1), n/a-n/a. https://doi.org/10.1029/2009GB003621

Fisher, R. A., Wieder, W. R., Sanderson, B. M., Koven, C. D., Oleson, K. W., Xu, C., et al. (2019). Parametric Controls on Vegetation Responses to Biogeochemical Forcing in the CLM5. *Journal of Advances in Modeling Earth Systems*, *11*(9), 2879–2895. https://doi.org/10.1029/2019MS001609

Ghimire, B., Riley, W. J., Koven, C. D., Mu, M., & Randerson, J. T. (2016). Representing leaf and root physiological traits in CLM improves global carbon and nitrogen cycling predictions. *Journal of Advances in Modeling Earth Systems*. https://doi.org/10.1002/2015MS000538

Kennedy, D., Swenson, S., Oleson, K. W., Lawrence, D. M., Fisher, R., Lola da Costa, A. C., & Gentine, P. (2019). Implementing Plant Hydraulics in the Community Land Model, Version 5. *Journal of Advances in Modeling Earth Systems*, *11*(2), 485–513. https://doi.org/10.1029/2018MS001500

Kim, H. (2017). Global Soil Wetness Project Phase 3 Atmospheric Boundary Conditions (Experiment 1). Data Integration and Analysis System (DIAS). https://doi.org/https://doi.org/10.20783/DIAS.501

Kriegler, E., Bauer, N., Popp, A., Humpenöder, F., Leimbach, M., Strefler, J., et al. (2017). Fossil-fueled development (SSP5): An energy and resource intensive scenario for the 21st century. *Global Environmental Change*, *42*, 297–315. https://doi.org/10.1016/j.gloenvcha.2016.05.015

Lawrence, D. M., Hurtt, G. C., Arneth, A., Brovkin, V., Calvin, K. V., Jones, A. D., et al. (2016). The Land Use Model Intercomparison Project (LUMIP) contribution to CMIP6: rationale and experimental design. *Geoscientific Model Development*, *9*(9), 2973–2998. https://doi.org/10.5194/gmd-9-2973-2016

Lawrence, D. M., Fisher, R. A., Koven, C. D., Oleson, K. W., Swenson, S. C., Bonan, G., et al. (2019). The Community Land Model Version 5: Description of New Features, Benchmarking, and Impact of Forcing Uncertainty. *Journal of Advances in Modeling Earth Systems*, *11*(12), 4245–4287. https://doi.org/10.1029/2018MS001583

NCAR. (2019). CLM5 Documentation Release, 337.

O'Neill, B. C., Tebaldi, C., Van Vuuren, D. P., Eyring, V., Friedlingstein, P., Hurtt, G., et al.

(2016). The Scenario Model Intercomparison Project (ScenarioMIP) for CMIP6. *Geoscientific Model Development*, *9*(9), 3461–3482. https://doi.org/10.5194/gmd-9-3461-2016

Öpik, M., Vanatoa, A., Vanatoa, E., Moora, M., Davison, J., Kalwij, J. M., et al. (2010). The online database MaarjAM reveals global and ecosystemic distribution patterns in arbuscular mycorrhizal fungi (Glomeromycota). *New Phytologist*, *188*(1), 223–241. https://doi.org/10.1111/j.1469-8137.2010.03334.x

Phillips, R. P., Brzostek, E., & Midgley, M. G. (2013). The mycorrhizal-associated nutrient economy: a new framework for predicting carbon-nutrient couplings in temperate forests. *New Phytologist*, *199*(1), 41–51. https://doi.org/10.1111/nph.12221

Read, D. J. (1991). Mycorrhizas in ecosystems. *Experientia*, *47*(4), 376–391. https://doi.org/10.1007/BF01972080

Reich, P. B., Sendall, K. M., Rice, K., Rich, R. L., Stefanski, A., Hobbie, S. E., & Montgomery, R. A. (2015). Geographic range predicts photosynthetic and growth response to warming in co-occurring tree species. *Nature Climate Change*, *5*(2), 148–152. https://doi.org/10.1038/nclimate2497

Riahi, K., van Vuuren, D. P., Kriegler, E., Edmonds, J., O'Neill, B. C., Fujimori, S., et al. (2017). The Shared Socioeconomic Pathways and their energy, land use, and greenhouse gas emissions implications: An overview. *Global Environmental Change*, *42*, 153–168. https://doi.org/10.1016/j.gloenvcha.2016.05.009

Shi, M., Fisher, J. B., Brzostek, E. R., & Phillips, R. P. (2016). Carbon cost of plant nitrogen acquisition: global carbon cycle impact from an improved plant nitrogen cycle in the Community Land Model. *Global Change Biology*, *22*(3), 1299–1314. https://doi.org/10.1111/gcb.13131

Soudzilovskaia, N. A., van Bodegom, P. M., Terrer, C., Zelfde, M. van't, McCallum, I., Luke McCormack, M., et al. (2019). Global mycorrhizal plant distribution linked to terrestrial carbon stocks. *Nature Communications*, *10*(1), 5077. https://doi.org/10.1038/s41467-019-13019-2

Steidinger, B. S., Crowther, T. W., Liang, J., Van Nuland, M. E., Werner, G. D. A., Reich, P. B., et al. (2019). Climatic controls of decomposition drive the global biogeography of forest-tree symbioses. *Nature*, *569*(7756), 404–408. https://doi.org/10.1038/s41586-019-1128-0

Sulman, B. N., Shevliakova, E., Brzostek, E. R., Kivlin, S. N., Malyshev, S., Menge, D. N. L., & Zhang, X. (2019). Diverse Mycorrhizal Associations Enhance Terrestrial C Storage in a Global Model. *Global Biogeochemical Cycles*, *33*(4), 501–523. https://doi.org/10.1029/2018GB005973

Tedersoo, L., Bahram, M., Põlme, S., Kõljalg, U., Yorou, N. S., Wijesundera, R., et al. (2014). Global diversity and geography of soil fungi. *Science*, *346*(6213), 1256688. https://doi.org/10.1126/science.1256688

Xu, C., Fisher, R., Wullschleger, S. D., Wilson, C. J., Cai, M., & McDowell, N. G. (2012). Toward a mechanistic modeling of nitrogen limitation on vegetation dynamics. *PLoS ONE*, *7*(5), 1–11. https://doi.org/10.1371/journal.pone.0037914